BIOCHEMISTRY
including biophysical chemistry & molecular biology

Article

pubs.acs.org/biochemistry

Assembly of Membrane-Bound Protein Complexes: Detection and Analysis by Single Molecule Diffusion

Brian P. Ziemba, Jefferson D. Knight,[†] and Joseph J. Falke*

Department of Chemistry and Biochemistry and the Molecular Biophysics Program, University of Colorado at Boulder, Boulder, Colorado 80309-0215, United States

ABSTRACT: Protein complexes assembled on membrane surfaces regulate a wide array of signaling pathways and cell processes. Thus, a molecular understanding of the membrane surface diffusion and regulatory events leading to the assembly of active membrane complexes is crucial to signaling biology and medicine. Here we present a novel single molecule diffusion analysis designed to detect complex formation on supported lipid bilayers. The usefulness of the method is illustrated by detection of an engineered, heterodimeric complex in which two membrane-bound pleckstrin homology (PH) domains associate stably, but reversibly, upon Ca^{2+}-triggered binding of calmodulin (CaM) to a target peptide from myosin light chain kinase (MLCKp). Specifically, when a monomeric, fluorescent PH-CaM domain fusion protein diffusing on a supported bilayer binds a dark MLCKp-PH domain fusion protein, the heterodimeric complex is observed to diffuse nearly 2-fold more slowly than the monomer because both of its twin PH domains can simultaneously bind to the viscous bilayer. In a mixed population of monomers and heterodimers, the single molecule diffusion analysis resolves, identifies and quantitates the rapidly diffusing monomers and slowly diffusing heterodimers. The affinity of the CaM-MLCKp interaction is measured by titrating dark MLCKp-PH construct into the system, while monitoring the changing ratio of monomers and heterodimers, yielding a saturating binding curve. Strikingly, the apparent affinity of the CaM-MLCKp complex is ~10^2-fold greater in the membrane system than in solution, apparently due to both faster complex association and slower complex dissociation on the membrane surface. More broadly, the present findings suggest that single molecule diffusion measurements on supported bilayers will provide an important tool for analyzing the 2D diffusion and assembly reactions governing the formation of diverse membrane-bound complexes, including key complexes from critical signaling pathways. The approach may also prove useful in pharmaceutical screening for compounds that inhibit membrane complex assembly or stability.

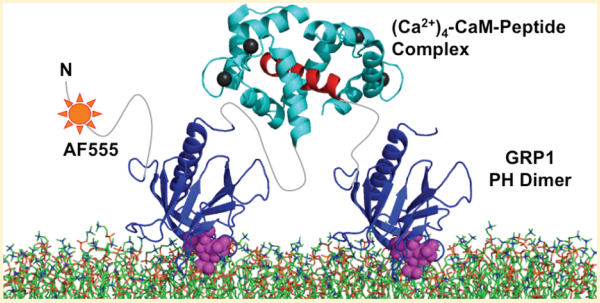

The lipid bilayers of cellular membranes provide two-dimensional platforms on which a diversity of multiprotein complexes are assembled to regulate essential cellular processes. Often, these complexes contain multiple, lipid-bound signaling proteins that together form molecular switches to activate or inhibit specific pathways. In general, assembly of the lipid-associated, multiprotein complex will be the rate-determining step in signal initiation or propagation, since signals can be rapidly transduced within the assembled complex. The ability to understand, and if possible control, complex formation on a molecular level would have significant biological and medical impacts.

The broad class of signaling pathways utilizing plasma membrane phosphatidylinositol-3,4,5-trisphosphate (PIP_3) as a second messenger illustrates the importance of lipid-associated, multiprotein complexes.[1−14] In such PIP_3-regulated pathways, signaling is often initiated by association of the plasma membrane lipid kinase phosphatide-3-kinase (PI3-kinase or PI3K) with a lipid-associated regulatory protein such as Ras. The resulting active, membrane-bound protein complex synthesizes PIP_3, which in turn recruits signaling proteins possessing PIP_3-specific pleckstrin homology (PH) domains to the plasma membrane surface. Often, the resulting PIP_3-associated signaling proteins interact with other lipid-bound proteins to form signaling complexes. For example, PDK1 (3-phosphoinositide-dependent protein kinase) and AKT1 (protein kinase B or PKB) both possess PIP_3-specific PH domains that are recruited to plasma membrane by a PIP_3 signal, thereby enabling the membrane-bound enzymes to associate and form an active complex in which PDK1 phospho-activates AKT1.[15−18] Subsequently, the active phospho-AKT1 regulates cell migration, cell growth, apoptosis, and other pathways. Hyperactivation of the PI3-kinase/PDK1/AKT1 signaling cascade stimulates cell growth and inhibits apoptosis, thereby inducing the development of human cancer and other diseases.[19,20]

Previous studies employing bulk or single molecule methods have shown that two-dimensional diffusion of membrane proteins is altered by formation of membrane-bound, protein−protein complexes. Studies in cells and supported lipid bilayers have employed fluorescence recovery after photobleaching (FRAP) to investigate membrane protein

Received: November 24, 2011
Revised: January 20, 2012
Published: January 21, 2012

diffusion and binding to transmembrane proteins or membrane-proximal cytoskeletal elements.[21−28] In two cases, membrane-bound monomers and covalent dimers yielded different diffusion coefficients, such that 2D diffusion of the dimer was signficantly slower.[28,29]

To our knowledge, however, no study has yet employed single molecule methods to detect the formation of noncovalent, membrane protein complexes on supported lipid bilayers by monitoring changes in two-dimensional diffusion rates. The present approach utilizes total internal reflection fluorescence (TIRF) microscopy to monitor single, engineered fusion proteins diffusing on a supported bilayer surface. Each fusion protein possesses a pleckstrin homology (PH) domain that binds tightly to the target lipid PIP_3. This PH domain is fused to either calmodulin (CaM) or a CaM target peptide from myosin light chain kinase (MLCKp). Complex formation is driven by the reversible, Ca^{2+}-triggered association of CaM with MLCKp,[30] yielding a heterodimer containing two PH domains.

The findings demonstrate that single molecule diffusion measurements enable sensitive detection of membrane protein complex formation. The heterodimeric PH-CaM/MLCKp-PH membrane complex diffuses more slowly than a monomeric fusion protein since the heterodimer can possess twice as many strong lipid contacts as the monomer. The single molecule diffusion behavior sheds light on the lipid contacts of the complex. Moreover, the single molecule analysis successfully resolves a mixture of monomers and complexes into their distinct subpopulations based on their contrasting diffusion rates and reveals the affinity of the membrane-bound complex when its fluorescent component is titrated with its dark binding partner. Notably, the affinity of the CaM-MLCKp interaction in the membrane system is 2 orders of magnitude higher than in solution because complex assembly is faster and disassembly is slower on the membrane surface. This important observation provides new insight into the role of biological membranes in facilitating protein complex formation and demonstrates the power of the single molecule approach to elucidate fundamental features of membrane surface reactions.

MATERIALS AND METHODS

Reagents. Synthetic phospholipids 1,2-dioleoyl-*sn*-glycero-3-phosphocholine (DOPC, PC), 1,2-dioleoyl-*sn*-glycero-3-phospho-L-serine (DOPS, PS), 1,2-dioleoyl-*sn*-glycero-3-phosphoinositol-3,4,5-trisphosphate [DOPI(3,4,5)P3, PI(3,4,5)P3], and 1,2-dioleoyl-*sn*-glycero-3-phosphoethanolamine-*N*-(lissamine rhodamine B sulfonyl) (LRB-DOPE, LRB-PE) were from Avanti Polar Lipids (Alabaster, AL). Alexa Fluor 555 (AF555) C2-maleimide was from Invitrogen (Carlsbad, CA). 2-Mercaptoethanol was from Fluka (Buchs, Germany). CoA trilithium salt was from Sigma (St. Louis, MO).

Construction of Vectors for Expression of GRP1 PH Fusion Proteins. DNA sequences encoding either human calmodulin (CaM, full length) or a human CaM-binding peptide (MLCKp, residues 212−234 of skeletal muscle myosin light chain kinase) were cloned into a vector previously generated in the Falke laboratory for expression of glutathione *S*-transferase fused to the human GRP1 PH domain (PH, residues 255−392).[8] To enable sequence-specific labeling with a CoA-linked fluorophore, oligonucleotides were synthesized (Integrated DNA Technologies, Coralville, IA) encoding the 11-amino acid recognition sequence for Sfp phosphopantetheinyl transferase[31] and were inserted just upstream of GRP1 PH in both expression vectors.[8] DNA sequencing confirmed the correct full sequence of both final constructs.

Protein Expression, Purification, and Labeling. All proteins were expressed in *E. coli* BL21 (DE3) as N-terminal glutathione *S*-transferase (GST) fusions and purified using glutathione affinity resin with thrombin cleavage as described previously.[8] Proteins were labeled with AF555 by Sfp enzyme using our published protocol.[29,31] Briefly, ∼2 μM target protein was incubated with 2.5 μM Alexa Fluor 555-CoA conjugate and 0.5 μM Sfp at room temperature for 2 h. Excess fluorophore was removed by buffer exchange in Vivaspin concentrators (Sartorius Stedim, Göttingen, Germany) until the flow-through was not visibly colored by AF555 absorption, and the flow-through was checked for absorbance at 555 nm. Concentration of labeled protein and labeling efficiency were determined from the measured absorbances of AF555 and intrinsic tryptophan residues.

Supported Lipid Bilayer Preparation. Supported lipid bilayers were prepared from sonicated unilamellar vesicles (SUVs) as described previously,[29,32] except that 0.5 mM Mg^{2+} was omitted from all buffers herein to minimize the possibility of Ca^{2+} contamination and ensure maximal Ca^{2+} regulation of the CaM construct. To make SUVs, the desired phospholipids were solubilized in chloroform:methanol:water (5:6:2) at the desired lipid molar ratio, and then the solvent was removed by vacuum prior to lipid rehydration with aqueous storage buffer (140 mM KCl, 15 mM NaCl, 0.02% NaN_3, 20 mM 2-mercaptoethanol, 25 mM HEPES, pH 7.5). The resulting aqueous lipid suspension (3.0 mM total lipid) was sonicated with a Misonix XL 2020 probe sonicator to produce sonicated, unilamellar vesicles that could be stored at 4 °C for up to 5 days before use. To make supported bilayers, glass coverslips (Pella, Redding, CA) were soaked for 1 h in piranha solution (3:1 H_2SO_4:H_2O_2), rinsed extensively with Milli-Q water, dried under a stream of N_2, and irradiated for 0.8 h in a Novascan PSD-UV ozone cleaner. A 60 μM perfusion chamber (Invitrogen, Eugene, OR) was adhered to each cleaned glass slide, and supported bilayers were formed via the vesicle fusion method using the SUVs described above.[8,29,32] The resulting bilayers were rinsed extensively with Milli-Q water and then exchanged into room temperature assay buffer (140 mM KCl, 15 mM NaCl, 5 mM reduced L-glutathione, 25 mM HEPES, pH 7.5) in preparation for TIRFM measurements.

TIRFM Measurements. TIRFM experiments were carried out on a home-built, objective-based TIRFM instrument, as described previously.[29,32] Supported lipid bilayers (described above) were imaged before and after addition of fluorescent protein. Typically, few fluorescent particles were observed on the bilayer prior to protein addition. After protein addition, samples were allowed to equilibrate 5 min to the ambient room temperature of 22 ± 1 °C. To minimize contributions from small numbers of immobile fluorescent particles (presumably inactive protein aggregates), a bleach pulse ∼30-fold higher power than used for imaging was applied for 2−5 s, and then fluorescence was allowed to recover for 60 s before data acquisition. Movie streams were acquired at a frame rate of 20 frames/s, and a spatial resolution of 7.0 pixels/μm, for each sample using MetaMorph software (AG Heinze). Subsequent particle tracking analysis was carried out using ImageJ,[33] and data processing and fitting were carried out using Mathematica (Wolfram Research) and GraphPad Prism 5 (GraphPad Software, Inc.).

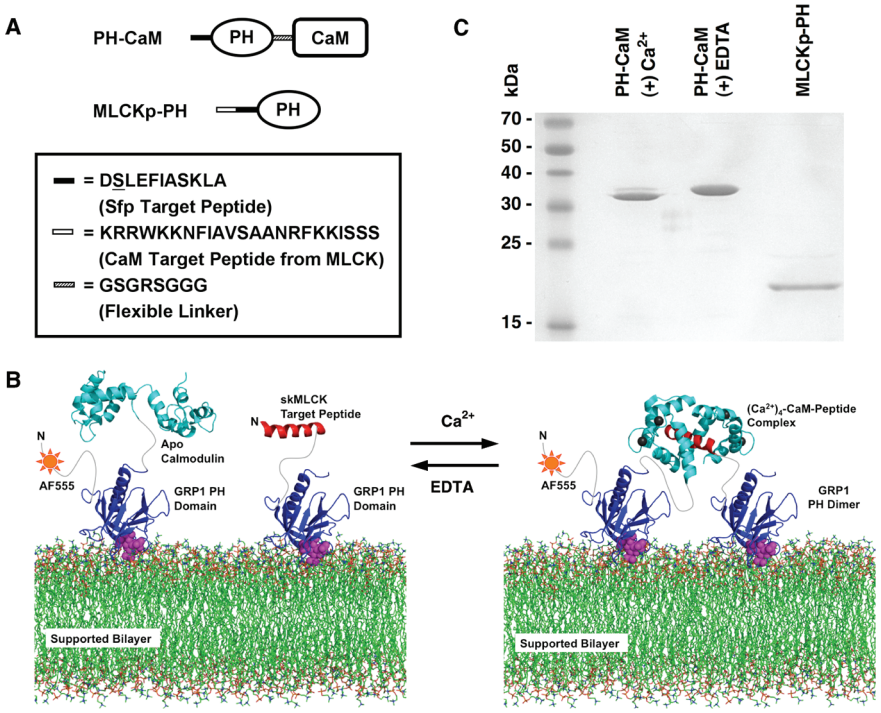

Figure 1. (A) Engineered PH domain fusion constructs used in this study. Schematic diagram illustrating the disposition of the individual fusion components: GRP1 PH domain (PH, residues 255−392), calmodulin (CaM), target peptide for CaM binding (CaM Target Peptide from skMLCK), target peptide for fluorophore coupling (Sfp Target Peptide), and flexible coupler between domains (Flexible Linker). (B) Design of the reversible membrane surface reaction between Fluor-PH-CaM and MLCKp-PH. Schematic structures utilize the known structures of individual domains and flexible linkers of appropriate lengths. IP_4-PH domain coordinates from PDB 1FGY,[41] Apo CaM coordinates from PDB 1DMO,[42] and $(Ca^{2+})_4$-CaM-MLCKp ternary complex coordinates from PDB 2K0F.[43] (C) SDS-PAGE analysis of the purified PH-CaM and MLCKp-PH fusion proteins. Migration of PH-CaM shifts with Ca^{2+} occupancy as previously noted for native CaM:[44] in the presence of Ca^{2+} most of the PH-CaM population is shifted (major band) while a minor subpopulation comigrates with the apo protein (minor band) as expected in the presence of SDS.

Single Particle Tracking. As in our previous studies,[29,32] diffusion trajectories of single fluorescent lipid and protein molecules were tracked and quantitated using the Particle Tracker plugin for ImageJ,[33] and then diffusion data were imported into Mathematica for further analysis. Briefly, the software determines the center position and intensity of each fluorescent particle in each frame and then links the particles in successive frames to form trajectories. Only particles possessing fluorescence intensities within a defined range were included in the analysis, thereby eliminating bright protein aggregates and dim, nonprotein contaminants. Additional exclusions removed immobile particles, rapidly dissociating particles, and overlapping tracks for which particle identity is lost. All exclusions were described and validated previously.[29,32]

Determination of Diffusion Coefficients from Single Molecule Data. Diffusion trajectory data were subjected to the one-component analysis described previously,[29,32] based on the method of Schütz et al.[34] For each set of processed trajectory data, we calculated the cumulative probability distribution $P(r^2,\Delta t)$ for square displacements of r^2 or greater over time interval Δt, where Δt ranged from 1 to 8 frames. For each value of Δt, the resulting distribution was best-fit to a single-component diffusion model:[34]

$$P(r^2, \Delta t) = 1 - e^{-r^2/\langle r^2\rangle} \quad (1)$$

yielding a best-fit mean-square displacement $\langle r^2\rangle$ for a given Δt. According to the 2-dimensional diffusion equation, the mean-square displacement is linearly related to Δt:

$$\langle r^2\rangle = 4D\Delta t \quad (2)$$

where D is the 2-dimensional diffusion coefficient. Finally, the linear least-squares, best-fit diffusion coefficient D was determined for a plot of $\langle r^2\rangle$ vs Δt.

Analysis of Multiple Diffusion Components in Heterogenous Populations. For mixed populations of monomeric proteins and complexes, the individual components were resolved using a combination of Mathematica and GraphPad Prism algorithms. For each individual track, an apparent diffusion coefficient was defined for that single diffusing particle by calculating its mean displacement between adjacent frames ($\langle r^2\rangle_{traj}$), which in turn was used to calculate the apparent diffusion coefficient D' for a single track:

$$\frac{\langle r^2\rangle_{traj}}{4\Delta t} = D' \quad (3)$$

Analyzing diffusing particles based on a Δt of one frame has been shown to underestimate the true diffusion coefficient by one-third;[35] thus, the true diffusion coefficient for a single track is $D = 3D'/2$. The resulting single track diffusion coefficients determined for large numbers of tracks were binned to generate a frequency distribution that, for a homogeneous population of diffusing particles, was found empirically to be well-fit by a Lorentzian function.

dx.doi.org/10.1021/bi201743a | *Biochemistry* 2012, 51, 1638−1647

Analysis of Complex Affinity by Titrating the Average Diffusion Coefficient of a Population. From the 2-dimensional diffusion equation (eq 2) it is straightforward to derive that the average diffusion coefficient of a mixed population of monomers and complexes is a simple weighted average of the monomer and complex diffusion coefficients ($D_{monomer}$ and $D_{complex}$, respectively), where the weighting factors are the fractions of the fluorescent particles in the monomer and complex subpopulations ($F_{monomer}$ and $F_{complex}$, respectively):

$$D_{average} = (D_{monomer}F_{monomer} + D_{complex}F_{complex}) \quad (4)$$

When the complex is formed by titration of one component into the system, in the present case by titrating the MLCKp-PH component into the system, the average diffusion coefficient of the population will yield a titration curve defined by

$$D_{average} = D_{monomer} + (D_{complex} - D_{monomer}) \times \frac{[\text{MLCKp-PH}]}{[\text{MLCKp-PH}] + K_{D(app)}} \quad (5)$$

where $D_{average}$ is the average population diffusion coefficient at a given concentration of MLCKp-PH and $K_{D(app)}$ is the apparent equilibrium dissociation constant for MLCKp-PH binding to the complex. Thus, the best-fit values of $K_{D(app)}$, $D_{monomer}$, and $D_{complex}$ can be determined by nonlinear least-squares fitting of a plot of $D_{average}$ vs [MLCKp-PH] with eq 5.

Statistics. Each diffusion coefficient in the text and tables is a mean ±1 SD determined from at least seven movies obtained in at least four separate experiments under identical conditions.

RESULTS

Strategy and Protein Constructs Employed. In a previous single molecule kinetic analysis of PH domain diffusion, we found that 2D diffusion rates of membrane-bound, PH domain constructs possessing different numbers of identical domains linked by flexible tethers (monomer, dimer, trimer) were inversely proportional to the number of tightly bound PIP_3 lipids.[29] The diffusion rates of these PH domain constructs were fully defined by the friction of the tightly bound PIP_3 lipids interacting with the highly viscous bilayer; by comparison, the friction between the protein and the aqueous phase was negligible. The findings suggested that kinetic analysis of single molecule diffusion would enable detection of complex formation between proteins on membrane surfaces, since the association of lipid-associated proteins would generate a complex possessing a larger number of bound lipids, more frictional drag, and slower diffusion than the individual proteins.

The present proof-of-concept study tests this prediction using the pair of engineered PH domain constructs illustrated in Figure 1A, designed to associate and form a heterodimer in a controlled and reversible fashion. In the PH-CaM construct the GRP1 PH domain (PH) is fused to calmodulin (CaM). In the MLCKp-PH construct the calmodulin target peptide from skeletal muscle myosin light chain kinase (MLCKp) is fused to GRP1 PH domain. The PH domain of each construct binds with high affinity to PIP_3 on a bilayer surface, and upon Ca^{2+} addition the Ca^{2+}-activated CaM protein will tightly bind the MLCKp target peptide, yielding a thermodynamically and kinetically stable heterodimer. Schematic Figure 1B illustrates the resulting reversible, membrane surface reaction. The 2D diffusion rate of this heterodimer bound to two PIP_3 molecules on the bilayer surface is predicted to be half that of a monomeric PH domain bound to a single PIP_3[29] and should be restored to the monomeric diffusion rate upon addition of excess Ca^{2+} chelator to reverse the CaM-MLCKp interaction.

For single molecule analysis of the effect of complex formation on 2D diffusion kinetics, the simplest approach monitors only one component of the complex. In contrast to multiprobe methods, such as FRET, this approach requires only a single fluorescent tag on the monitored component, thereby preventing perturbations or complications arising from a second probe. The surface diffusion of the fluor-tagged component is quantitated while increasing the surface density of dark components, thereby titrating the assembly reaction. When desired, all of the fluorescent component can be driven into the complex by addition of saturating dark component(s). The present study utilizes a fluor-tagged CaM fusion construct and a dark MLCKp fusion construct (Figure 1A).

Isolation and Characterization of Protein Constructs. Expression plasmids were created for the PH-CaM and MLCKp-PH constructs fused to GST, then both fusions were expressed in *E. coli*, isolated by GST-tag affinity purification, and the GST-tag was removed by proteolysis (Materials and Methods). SDS-PAGE analysis of the resulting PH-CaM and MLCKp-PH proteins indicates their purity exceeds 95% (Figure 1C). Where appropriate, a given construct was tagged with Alexa Fluor 555 (AF555) by enzymatic labeling with Sfp (Materials and Methods[29,31]). To ascertain whether the resulting proteins retained the native specificity for PIP_3 lipid in the membrane targeting reaction, the binding of each fluorescent construct to 3:1 PC:PS supported bilayers lacking or containing PIP_3 (lipid compositions in Table 1) was analyzed by single molecule TIRF microscopy. Figure 2 shows that, like native GRP1 PH domain, both the PH-CaM and MLCKp-PH constructs require PIP_3 for supported bilayer binding (Figure 2A). In addition, the PIP_3 affinities of the two fusion constructs and the isolated PH domain are all similar, since each yields a similar surface density of membrane-bound fluorescent molecules when added to PIP_3-containing supported bilayers at the same subsaturating concentration (50 pM total) (Figure 2A). The density of bound protein is extremely low under these conditions: an average TIRF field contains ~1.4×10^9 total lipids in the exposed monolayer, of which ~2.8×10^7 are PIP_3 lipids. Only ~160 of these PIP_3 lipids are occupied by PH domain, representing 5 ppm of the exposed PIP_3 population. Finally, binding of the fusion constructs to the target bilayer is unaltered, within error, by addition of Ca^{2+} (Figure 2B). Thus, in both the CaM and MLCK fusion constructs, GRP1 PH domain retains its native, PIP_3-specific membrane binding, and the presence of Ca^{2+} does not significantly affect this interaction.

Table 1. Lipid Compositions of Supported Bilayers

mixture	lipid (mol %)
PC:PS	75:25
PC:PS:PIP_3	74:24:2
PC:PS:PIP_3 (+) LRB-PE	74:24:2 (+) 200 ppb

Analysis of Membrane Complex Formation by Single Molecule Diffusion. As we have previously shown, single molecule TIRF enables highly quantitative diffusion analysis of

dx.doi.org/10.1021/bi201743a | *Biochemistry* 2012, 51, 1638–1647

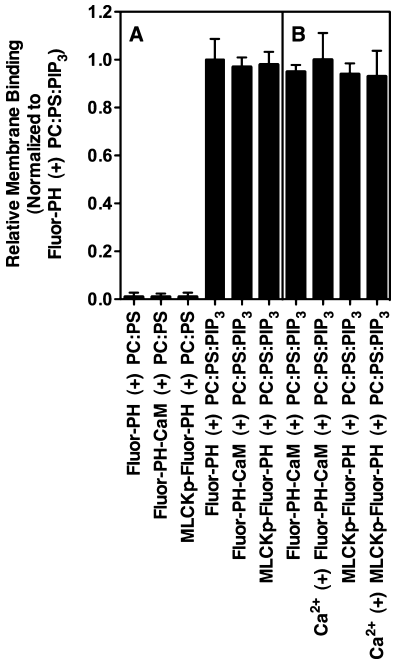

Figure 2. Single molecule TIRF quantitation of fluorescent protein binding to supported bilayers. All constructs were added to the imaging chamber containing a standard supported bilayer (3:1 PC:PS (+) 2% PIP_3) at the same total concentration (50 pM), and then the density of fluorescent protein binding per unit area was quantitated. (A) Omission of PIP_3 from the bilayer virtually eliminates membrane binding, confirming the binding is PIP_3-specific. (B) Addition of 50 μM Ca^{2+} does not alter protein binding to the membrane.

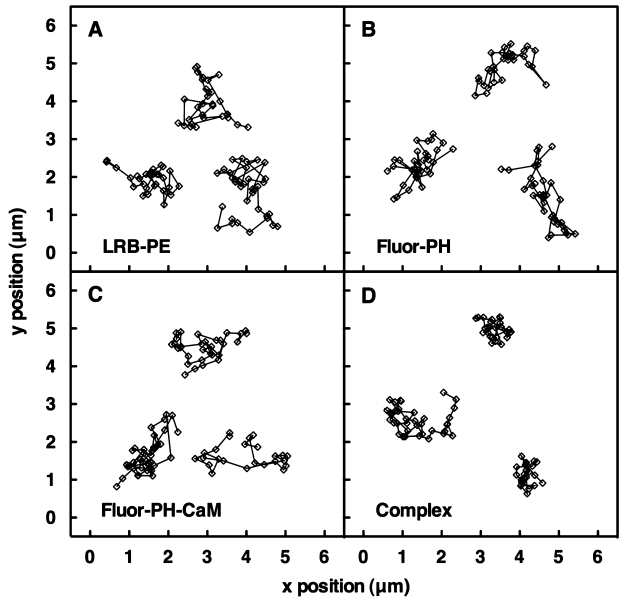

Figure 3. Representative single particle tracks of freely diffusing fluorescent particles on standard supported bilayers at 22 °C: (A) LRB-PE, (B) Fluor-PH domain, (C) Fluor-PH-CaM fusion protein, and (D) complex formed between Fluor-PH-CaM and saturating MLCKp-PH. Shown are 20 ms single steps as captured by the 50 s^{-1} frame rate. Formation of the heterodimeric Fluor-PH-CaM/MLCK-PH complex clearly slows diffusion.

fluorescent proteins bound to supported bilayers.[29,32] The present study compared the diffusion of three monomeric, membrane-bound fluorescent molecules: (i) PH-CaM fusion protein labeled with AF555 (AF555-PH-CaM) and bound to PIP_3; (ii) isolated PH domain labeled with AF555 (A555-PH) and bound to PIP_3; and (iii) fluorescent lipid labeled on its headgroup with Lissamine Rhodamine B (LRB-PE) and incorporated into the bilayer. To investigate reversible complex formation, the study also investigated the diffusion of the AF555-labeled PH-CaM fusion protein in the presence of saturating Ca^{2+} and dark MLCK-PH fusion protein. All diffusion experiments utilized supported bilayers composed of 3:1 PC:PS with 2 mol % PIP_3. For each experimental condition, multiple TIRF movies were collected and analyzed with particle tracking software as previously described,[29,32] together yielding a large number of single particle diffusion tracks. Subsequent data processing (Materials and Methods) eliminated the tracks of immobile particles, which represented only a small fraction (1 ± 1% averaged over all movies, never more than 4% in a given movie) of the particle population and arose from defective particle interactions. (As previously discussed, defective interactions could involve glass spikes that penetrate the bilayer, small zones of defective bilayer, and/or non-native binding of unfolded or aggregated proteins to the bilayer.[29,32]) Thus, the final data analysis focused solely on the dominant subpopulation of freely diffusing molecules with native bilayer interactions.

Figure 3A–D displays representative particle tracks of freely diffusing particles and complexes. It is evident that complexes diffuse more slowly. To extract and summarize the diffusion information from multiple movies for a given condition containing hundreds of tracks and thousands of individual steps, these thousands of steps were used to define an ensemble wherein the individual step lengths and times are known. Subsequently the features of the ensemble were analyzed to ascertain whether the population was homogeneous and to measure the characteristic parameters of the population. Note this approach employing single molecule data is opposite the standard approach of bulk methods in which bulk quantities are measured and the statistics of the ensemble are modeled based on assumptions about the nature of the ensemble. Here the statistics of the ensemble are known and analyzed rather than inferred from an assumed model.

Figure 4A–D presents semilog plots of probability vs minimum square displacement, which for the exponential behavior of a homogeneously diffusing population of particles will yield a straight line.[29,32] For the monomeric LRB-PE fluorescent lipid, AF555-PH domain, and AF555-PH-CaM fusion, the observed data are well fit by straight lines and the diffusion is homogeneous. Moreover, the monomeric PH domain constructs exhibit virtually the same diffusion rate as the monomeric lipid (compare solid and dashed lines in Figure 4B,C). For the complex between Ca^{2+}, AF555-PH-CaM, and MLCKp-PH, however, the diffusion is significantly slower and deviates from linear, homogeneous behavior with large step sizes exhibiting higher than expected probabilities (Figure 4D). The simplest explanation for the deviation is that as the complex diffuses, one of the two PH domains of the heterodimer transiently dissociates from the bilayer, enabling the fluorescent AF555-PH-CaM component to occasionally "skate" on a single PH domain-PIP_3 contact (see Discussion). Finally, Figure 5A presents standard diffusion plots of mean-square displacement vs time interval for the monomeric particles and the complex. Here the monomeric particles and the complex all exhibit the linear behavior predicted for

dx.doi.org/10.1021/bi201743a | *Biochemistry* 2012, 51, 1638–1647

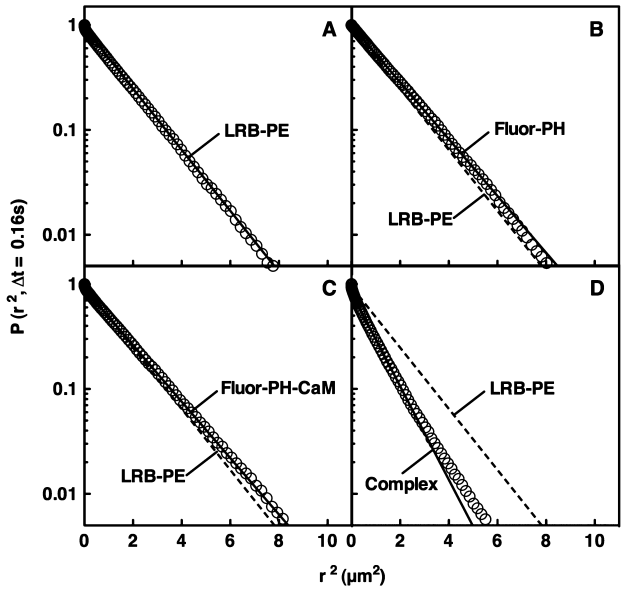

Figure 4. Plots of probability (P) vs minimum square displacement (r^2) for particles diffusing on standard supported bilayers at 22 °C. The vertical axis represents the probability of a particle possessing a square displacement of at least r^2 in images acquired 8 frames apart (20 ms per frame). The solid best-fit straight line illustrates the exponential behavior expected for homogeneous diffusion. Shown are plots for (A) LRB-PE, (B) Fluor-PH domain, (C) Fluor-PH-CaM, and (D) Fluor-PH-CaM in complex with saturating dark MLCKp-PH and Ca^{2+}. Each plot was compiled from at least 900 single particle tracks gathered from three or more movies.

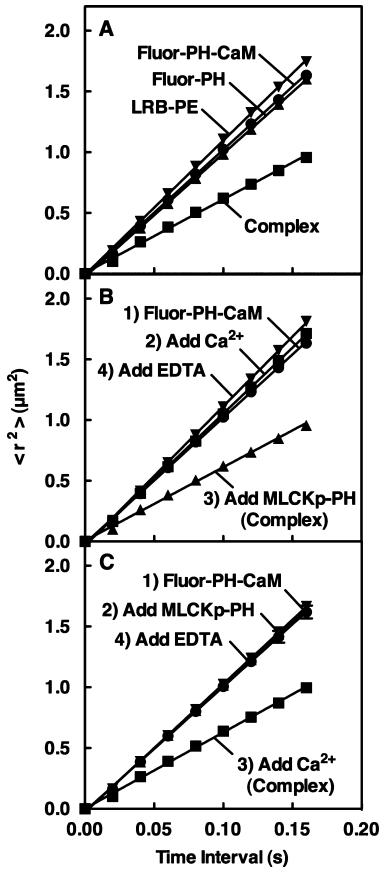

Figure 5. Plots of mean-square displacement $\langle r^2 \rangle$ vs time interval for particles diffusing on standard supported bilayers at 22 °C. For each type of particle or condition the solid best-fit straight line defines the diffusion coefficient as summarized in eq 2 and Table 1. (A) Comparison of monomeric lipid diffusion, monomeric protein diffusion, and heterodimeric protein diffusion (same data as in Figure 4). (B, C) Comparison of Fluor-PH-CaM diffusion upon addition of reagents in the indicated order. Each plot was compiled from at least 900 single particle tracks gathered from three or more movies.

unrestricted diffusion in two dimensions ($\langle r^2 \rangle = 4D\Delta t$, eq 2).[29,32] The high quality of the data enables accurate determination of the diffusion coefficient from the best-fit slope, and Table 2 summarizes the resulting diffusion coefficients. The linearity observed for the complex does not contradict the evidence above (Figure 4D) that the complex exhibits both slowly diffusing and rapidly diffusing states, since a heterogeneous population can yield a linear diffusion plot (see eq 4 of Materials and Methods and the final section of Results).

The diffusion plots of Figure 5B,C illustrate the effect of protein−protein complex assembly on the diffusion kinetics of the AF555-PH-CaM construct. To test whether the diffusion behavior of the complex is independent of the order of Ca^{2+} and MLCKp-PH addition, two different assembly protocols were utilized. The first protocol began with (i) the AF555-PH-CaM construct bound to PIP_3 on the supported bilayer, then (ii) saturating Ca^{2+} was added, followed by (iii) saturating dark MLCKp-PH construct, and finally (iv) excess EDTA. Each of these conditions yields a linear diffusion plot in Figure 5B, where the observed slopes (and thus diffusion coefficients) are similar to that of the monomeric AF555-PH-CaM construct except when the slowly diffusing complex forms in the presence of saturating Ca^{2+} and dark MLCKp-PH. Upon complex formation, the diffusion coefficient of the monomeric AF555-PH-CaM construct ($D = 2.5 \pm 0.1$ μm^2 s^{-1}) drops significantly to a lower value ($D = 1.5 \pm 0.1$ μm^2 s^{-1}). This 40% decrease is close to the 50% decrease in diffusion coefficient expected[29] for conversion of the monomeric construct to a heterodimeric complex. In the second protocol the Ca^{2+} was added after the dark MLCKp-PH construct. Again, each condition yields a linear diffusion plot with the slope characteristic of the monomeric AF555-PH-CaM construct except when the slowly moving complex forms in the presence of saturating Ca^{2+} and dark MLCKp-PH (Figure 5C). As in the other protocol, the diffusion coefficient of the complex is decreased 40% relative to the monomeric AF555-PH-CaM construct. In both protocols, chelation of Ca^{2+} by excess EDTA triggers dissociation of the complex and restores the more rapid monomeric diffusion (Figure 5B,C).

Table 2 also presents the results of control experiments testing alternative explanations for the slowing of AF555-PH-CaM diffusion upon complex formation with Ca^{2+} and MLCKp-PH. As noted above, the diffusion coefficient of fluorescent, membrane-bound AF555-PH-CaM is not altered by addition of Ca^{2+} alone, nor by MLCK-PH alone, nor by both components in the presence of excess EDTA, consistent with the conclusion that diffusional slowing requires ternary complex formation between all three components. The CaM-MLCKp interaction is essential since the diffusion coefficient of AF555-PH-CaM is not changed by addition of isolated, dark GRP1 PH domain lacking the MLCKp target peptide in the presence of saturating Ca^{2+} (Table 2). Finally, no significant change in the diffusion coefficient of fluorescent lipid is observed upon addition of Ca^{2+}, dark PH-CaM, or dark MLCKp-PH in any

dx.doi.org/10.1021/bi201743a | Biochemistry 2012, 51, 1638−1647

Table 2. Summary of Diffusion Coefficients Measured by Single Molecule Analysis[a]

additions to supported bilayer (PC:PS:PIP_3)	D ($\mu m^2/s$)
200 ppb LRB-PE (lipid)	2.6 ± 0.1
50 pM Fluor-PH-CaM	2.5 ± 0.1
50 pM Fluor-PH-CaM (+) 50 μM Ca^{2+}	2.5 ± 0.1
50 pM Fluor-PH-CaM (+) 1.5 nM MLCKp-PH	2.5 ± 0.1
50 pM Fluor-PH-CaM (+) 1.5 nM MLCKp-PH (+) 50 μM Ca^{2+}	1.5 ± 0.1
50 pM Fluor-PH-CaM (+) 1.5 nM MLCKp-PH (+) 50 μM Ca^{2+} (+) 100 μM EDTA	2.6 ± 0.2
50 pM Fluor- PH-CaM (+) 1.5 nM PH	2.5 ± 0.1
50 pM Fluor-PH	2.7 ± 0.1
50 pM Fluor-PH (+) 1.5 nM MLCKp-PH	2.4 ± 0.1
200 ppb LRB-PE (+) 50 pM PH-CaM	2.7 ± 0.1
200 ppb LRB-PE (+) 50 pM PH-CaM (+) 50 μM Ca^{2+}	2.7 ± 0.1
200 ppb LRB-PE (+) 50 pM PH-CaM (+) 50 μM Ca^{2+} (+) 1.5 nM MLCKp-PH	2.7 ± 0.1
200 ppb LRB-PE (+) 50 pM PH-CaM (+) 50 μM Ca^{2+} (+) 1.5 nM MLCKp-PH (+) EDTA	2.7 ± 0.2

[a]LRB-PE (fluor-labeled lipid), Fluor-PH-CaM (fluor-labeled PH domain-CaM fusion protein), PH-CaM (dark PH domain-CaM fusion protein), MLCKp-PH (dark MLCKp-PH domain fusion protein containing the CaM-binding peptide from skeletal muscle myosin light chain kinase), Fluor-PH (fluor-labeled PH domain), PH (dark PH domain; in all cases herein PH is the GRP1 PH domain).

combination. It follows that the slowing of AF555-PH-CaM diffusion upon addition of saturating Ca^{2+} and dark MLCKp-PH complex arises solely from the formation of the stable ternary complex, which experiences diffusional slowing due to its twin PH domain contacts with bilayer-associated PIP_3 molecules.

The present study was carried out in the absence of Mg^{2+} to minimize the Ca^{2+} contamination present in commercial Mg^{2+}, thereby providing a low Ca^{2+} background for CaM regulation. Under these Mg^{2+}-free conditions, the rates of fluorescent PH domain and fluorescent lipid diffusion on PC:PS:PIP_3 bilayers are the same, within error (Table 2). By contrast, our previous study carried out in the presence of Mg^{2+} found that fluorescent PH domain diffuses ~30% more slowly than fluorescent lipid on bilayers containing PS.[32] Additional studies (Ziemba and Falke) have confirmed that, in contrast to Ca^{2+} (Table 2), Mg^{2+} slows PH domain diffusion on target membranes containing PS. Further work is required to elucidate the mechanism of this Mg^{2+}-specific, PS-specific effect.

Titration To Define the Affinity of the Membrane Complex. The equilibrium affinity of the membrane-associated $(Ca^{2+})_4$-CaM-MLCKp complex could differ significantly from that of soluble $(Ca^{2+})_4$-CaM-MLCKp complex if the membrane interactions alter the complex assembly or disassembly rate. Thus, it would be interesting to compare the affinity of the membrane-associated ternary complex with the known affinity of the soluble ternary complex.[30,36]

Because of the linearity of the diffusion equation ($\langle r^2 \rangle = 4D\Delta t$, eq 2), the macroscopic diffusion coefficient exhibited by an ensemble of single molecule steps taken by a mixture of monomers and heterodimeric complexes is simply the average of the microscopic diffusion coefficients of the two types of particles, weighted by the fractional population of each component (eq 4). The dependence of this average diffusion coefficient ($D_{average}$) on fractional populations, in turn, enables a simple titration experiment to determine the apparent equilibrium dissociation constant for complex assembly ($K_{D(app)}$, eq 5). The average diffusion coefficient of membrane-bound AF555-PH-CaM was quantitated while increasing concentrations of dark MLCKp-PH construct were titrated into the system at a fixed, saturating [Ca^{2+}]. Figure 6 shows the resulting titration curve, which when best-fit by eq 5 for homogeneous sites yields $K_{D(app)}$ = 39 ± 9 pM. By contrast, K_D estimates for the soluble complex range from 1 to 20 nM at saturating [Ca^{2+}]. Thus, in the present membrane system a ~10^2-fold lower concentration of MLCKp construct is needed to half-saturate the CaM construct than observed for MLCKp half-saturation of CaM in solution. It follows that the membrane interactions of the present constructs greatly enhance the stability of the $(Ca^{2+})_4$-CaM-MLCKp ternary complex.

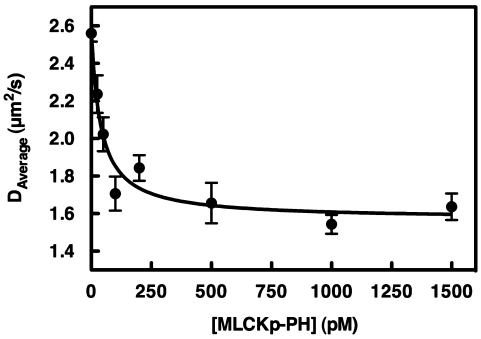

Figure 6. Titration of Fluor-PH-CaM with dark MLCKp-PH in the presence of saturating Ca^{2+} on standard supported bilayers at 22 °C. The solid curve represents the nonlinear least-squares best fit of the titration data with eq 5, which defines the relationship between the average diffusion coefficient for a mixed monomer−heterodimer population and the bulk free concentration of MLCKp-PH. The resulting best-fit apparent equilibrium dissociation constant is $K_{D(app)}$ = 39 ± 9 pM. Each $D_{average}$ at a given [MLCKp-PH] was defined by at least 1000 single particle tracks gathered from three or more movies.

At subsaturating concentrations of MLCKp-PH, the AF555-PH-CaM population consists of two subpopulations: the AF555-PH-CaM monomer and the heterodimeric complex of AF555-PH-CaM with MLCK-PH. The bound-state lifetime of the $(Ca^{2+})_4$-CaM-MLCK complex in solution is long (>10 s[36]) compared to lifetime of typical AF555-PH-CaM diffusion tracks on supported bilayers (1−10 s), suggesting that a bilayer-associated population may exhibit resolvable fast tracks for monomers and slow tracks for heterodimers. Thus, a diffusion coefficient was estimated for each single particle track (Materials and Methods), and distributions of single track diffusion coefficients were compiled as illustrated in Figure 7. When the fluorescent AF555-PH-CaM population is fully monomeric (Figure 7A, absence of MLCKp-PH) or fully heterodimeric (Figure 7B, saturating MLCKp-PH), the distribution is well fit by a Lorentzian function in which the most probable diffusion coefficient is the same, within error, as the diffusion coefficient measured by standard analysis (Figure 5 and Table 2). When the population is a mixture of monomers and heterodimers, the data are well fit by a two-component model in which two Lorentzians are observed for the pure populations in different ratios (Figure 6C, in this case 24% monomers and 76% heterodimers). Thus, the single molecule approach enables both resolution and quantitation of the different oligomeric species in a heterogeneous population of membrane-associated proteins.

dx.doi.org/10.1021/bi201743a | Biochemistry 2012, 51, 1638−1647

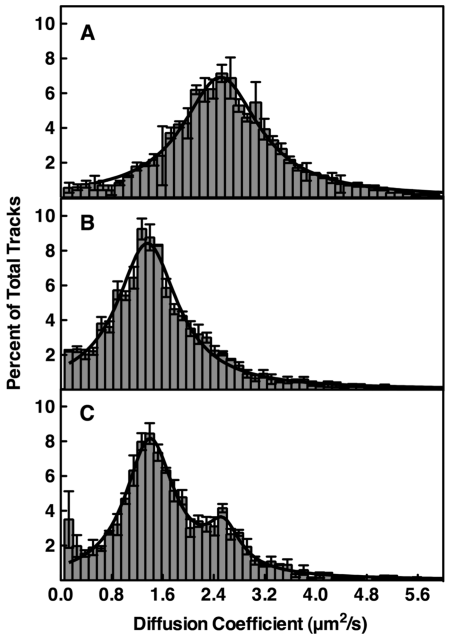

Figure 7. Distributions of single track diffusion coefficients on standard supported bilayers at 22 °C. For each Fluor-PH-CaM diffusion track, a diffusion coefficient was determined by eq 3, and the resulting single track diffusion coefficients were binned as shown. Homogeneous populations of (A) monomeric Fluor-PH-CaM or (B) heterodimeric Fluor-PH-CaM/MLCKp-PH complex yielded single Lorentzian distributions, while (C) a mixture of the monomeric and heterodimeric species yielded two resolved Lorentzian distributions, one for each subpopulation. In each figure the bold curve is the best-fit single or double Lorentzian. Each distribution was compiled from at least 1000 single particle tracks gathered from three or more movies.

Other methods such as FRAP and FRAPP can also resolve multiple diffusion coefficients in a heterogeneous population if the diffusion rates are sufficiently different.[37] However, unlike the current approach, these methods do not directly measure the distribution of diffusion coefficients for individual particles (Figure 7). In addition, these methods have difficulty distinguishing diffusion on membrane from diffusion through solution, while the current approach focuses solely on membrane diffusion. Thus, the interpretation of FRAP and FRAPP ensemble data may often be more complicated and model-dependent than the interpretation of single molecule data.

DISCUSSION

The present findings demonstrate that single molecule diffusion studies can detect the formation of membrane-associated complexes between lipid-bound proteins. Our previous studies have shown that the two-dimensional diffusion of GRP1 PH domain bound to its target PIP_3 lipid on a bilayer surface is dominated by the interactions of the PIP_3 with the bilayer[32] and that the diffusion coefficient of PH domains chained together by flexible linkers is proportional to $1/N$, where N is the number of PIP_3 molecules tightly bound in the complex.[29] As predicted by this inverse relationship between the diffusion coefficient and the number of tightly bound lipids, the present study finds that conversion of a monomeric PH domain construct to a noncovalent, heterodimeric PH domain complex decreases its diffusion coefficient nearly 2-fold, such that $D_{complex} = 0.6D_{monomer}$ (Table 2 and Figure 5A–C). Closer inspection reveals that the complex diffuses slightly but reproducibly faster than expected for a dimer ($D_{dimer} = 0.5D_{monomer}$), and this discrepancy is consistent with the observed deviation of the complex from homogeneous diffusion on a plot of probability vs minimum square displacement (Figure 4D). The simplest explanation for both anomolies is that the heterodimeric complex can exhibit two membrane binding modes: a predominant, slowly diffusing "twin binding" mode in which both PH domains are simultaneously bound to bilayer-associated PIP_3 molecules and a transient, more rapidly diffusing "skating" mode in which diffusion is constrained by only one PH–PIP_3 interaction. Mechanisms by which skating could occur include (i) transient dissociation of one PH domain from the bilayer within the stable heterodimer and (ii) transient dissociation of the heterodimer into its monomeric components. Assuming that the macroscopic diffusion coefficient of the complex is a weighted average of the microscopic diffusion coefficients for twin binding mode ($D_{twin} = 0.5D_{monomer}$) and for skating mode ($D_{skating} = D_{monomer}$), eq 4 indicates the complex spends ~80% of its time in twin binding mode.

The noncovalent interaction employed to stabilize the heterodimeric complex, namely the Ca^{2+}-triggered binding of CaM to its MLCK target peptide, is kinetically stable with a lifetime of tens of seconds in the presence of saturating Ca^{2+}.[36] Because of this stability, under subsaturating conditions the diffusion tracks of rapidly moving monomers and slowly moving heterodimers can be resolved, and their fractional populations can be directly determined. Moreover, the average diffusion coefficient of a mixture of monomers and heterodimers is a weighted average of their distinct microscopic diffusion coefficients (eq 4); thus, measurement of the average diffusion coefficient for the AF555-PH-CaM population during a titration with dark MLCKp-PH allows quantitation of the changing ratio of monomeric and oligomeric particles, thereby revealing the oligomer affinity (eq 5).

Strikingly, the apparent affinity of the $(Ca^{2+})_4$-CaM-MLCKp complex is ~10^2-fold higher in the present membrane system than observed for the analogous $(Ca^{2+})_4$-CaM-MLCKp complex in solution.[30] In principle, the enhanced affinity observed for the present system could arise from an increased rate of complex assembly on the membrane surface, owing to more frequent collisions between components recruited to the membrane where effective density can be greater and where diffusion occurs in two dimensions rather than three. Alternatively, the affinity increase could arise from slower dissociation of the membrane-bound complex owing to the stabilization provided by association of each PH domain with PIP_3 and by the high bilayer viscosity, both of which would slow the diffusional separation of the components following a microdissociation event, thereby increasing the probability of rebinding. Less likely to contribute are the geometric effects of membrane association on complex assembly, since the long, flexible linkers between the binding partners and their PH domains enable CaM and MLCKp to undergo rapid, random tumbling relative to each other much like they experience when associating in solution.

To investigate the possibility that faster complex assembly contributes to the membrane-associated affinity increase, one can compare the collision rates predicted for complex formation on the membrane surface and in solution.[38] The 2D collision rate can be calculated from the known parameters for conditions that yield ~50% occupancy of the PIP_3-bound

dx.doi.org/10.1021/bi201743a | *Biochemistry* 2012, 51, 1638–1647

CaM construct with PIP_3-bound MLCKp construct on the supported bilayer (50 pM total each construct in the diffusion chamber, saturating Ca^{2+}, standard PC:PS:PIP_3 target membrane; together these conditions yield a protein density of 0.2 monomers μm^{-2}, a monomer 2D diffusion coefficient of 2 μm^2 s^{-1} and a monomer collision radius of 2×10^{-4} μm). Insertion of these parameters into the 2D collision rate calculation[38] suggests that each membrane-bound CaM construct will experience collisions with membrane-bound MLCKp constructs at a rate of ~0.8 collisions s^{-1}, which may underestimate the true complex formation rate since it ignores complexes formed in solution that subsequently dock to the membrane. The 3D collision rate between Ca^{2+}-saturated CaM and MLCK peptide in solution can be calculated[38] for the same reaction conditions omitting the membrane (50 pM each component, saturating Ca^{2+}, 22 °C; together these conditions yield a monomer 3D diffusion coefficient of 80 μm^2 s^{-1} for CaM and 110 μm^2 s^{-1} for MLCK peptide, as well as a monomer collision radius of 3×10^{-4} μm for CaM and 2×10^{-4} μm for MLCK peptide[39]). The resulting 3D calculation predicts that each Ca^{2+}-saturated CaM molecule in solution will collide with MLCK peptides at a rate ~6-fold slower than predicted for the membrane system, suggesting that the rate of complex assembly is significantly slower in solution than on the membrane surface. It follows that the higher particle density and/or reduced dimensionality of the membrane system speeds complex assembly.

Notably, the ~6-fold collision rate enhancement predicted for the membrane system does not fully explain the observed ~10^2-fold affinity enhancement. Instead, the slowing of complex dissociation by membrane contacts may play an even larger role. It would not be surprising if slower dissociation is the dominant factor due to the strong caging effects of the PH domain−bilayer interactions that prevent rapid diffusion of the dissociating CaM and MLCKp components. Further study is needed to quantitate the relative contributions of faster assembly rates and slower disassembly rates.

The present proof-of-concept study demonstrates the feasibility of using single molecule diffusion kinetics to detect the formation of membrane protein complexes on supported lipid bilayers. We expect this approach will be widely useful in studies of bilayer-associated complexes formed between membrane proteins. Diffusional analysis of membrane complex formation can, in favorable cases, be carried out in cells; however, a major advantage of the present *in vitro* approach is the ability to vary the lipid composition of supported bilayers in a controlled, strategic manner.[29,32] The resulting systematic analysis of lipid contributions can elucidate the roles of specific lipids in membrane targeting, complex formation, and complex activity. Moreover, the single molecule diffusion analysis can yield a wealth of information difficult to obtain in bulk experiments, such as resolution of multiple diffusion states arising from distinct assembly intermediates or heterogeneous populations of stable complexes.

The ability to directly monitor 2D diffusion and membrane complex formation has important biological and medical applications. For example, many signaling proteins possess lipid targeting domains (PH, C1, C2, FYVE, ENTH, ANTH, others) that bind to target lipids on a specific intracellular membrane.[10,12,40] Typically, the function of this membrane targeting is to bring the signaling protein into the proximity of other membrane-bound signaling proteins, thereby enabling 2D diffusion and collisional formation of an active membrane complex that controls essential cell processes. It follows that a molecular understanding of membrane surface diffusion and membrane complex formation is crucial to signaling biology. *In vitro* single molecule analysis of membrane protein diffusion will provide both (i) a new window into the basic assembly mechanisms of membrane-bound protein complexes and (ii) a sensitive assay for complex formation suitable for automation and screening of inhibitors that disrupt complex assembly and stability.

AUTHOR INFORMATION

Corresponding Author

*E-mail falke@colorado.edu; Tel (303) 492-3503; Fax (303) 492-5894.

Present Address

[†]Department of Chemistry, University of Colorado, Denver, CO 80217-3364.

Funding

Support was provided by NIH R01 GM-063235 (to J.J.F.).

Notes

The authors declare no competing financial interest.

ACKNOWLEDGMENTS

The authors thank Prof. Amy Palmer for the use of plasmid constructs containing calmodulin and its myosin light chain kinase target sequences as well as Prof. Arthur Pardi and the W. M. Keck Single Molecule facility at University of Colorado, Boulder, for TIRF instrumentation and members of the Falke group (Annette Erbse, Kene Piasta, Peter Slivka) for helpful comments on the manuscript.

ABBREVIATIONS

PH domain, pleckstrin homology domain; CaM, calmodulin; MLCKp, CaM-binding peptide from skeletal muscle myosin light chain kinase; Sfp, phosphopantethienyl transferase; AF555, Alexa Fluor 555; PC, phosphatidylcholine 1,2-dioleoyl-*sn*-glycero-3-phosphocholine; PS, phosphatidylserine 1,2-dioleoyl-*sn*-glycero-3-phospho-L-serine; $PI(3,4,5)P_3$ or PIP_3, phosphatidylinositol-3,4,5-trisphosphate 1,2-dioleoyl-*sn*-glycero-3-phosphoinositol-3,4,5-trisphosphate; LRB-PE, 1,2-dioleoyl-*sn*-glycero-3-phosphoethanolamine-*N*-[lissamine rhodamine B sulfonyl]; SUV, sonicated unilamellar vesicle; DTT, dithiothreitol; EDTA, ethylenediaminetetraacetic acid; TIRF, total internal reflection fluorescence microscopy; FRAP, fluorescence recovery after photobleaching; GST, glutathione *S*-transferase.

REFERENCES

(1) Lemmon, M. A., and Ferguson, K. M. (2000) Signal-dependent membrane targeting by pleckstrin homology (PH) domains. *Biochem. J. 350* (Pt. 1), 1−18.

(2) Czech, M. P. (2000) PIP2 and PIP3: complex roles at the cell surface. *Cell 100*, 603−606.

(3) Insall, R. H., and Weiner, O. D. (2001) PIP3, PIP2, and cell movement--similar messages, different meanings? *Dev. Cell 1*, 743−747.

(4) Vanhaesebroeck, B., Leevers, S. J., Ahmadi, K., Timms, J., Katso, R., Driscoll, P. C., Woscholski, R., Parker, P. J., and Waterfield, M. D. (2001) Synthesis and function of 3-phosphorylated inositol lipids. *Annu. Rev. Biochem. 70*, 535−602.

(5) Wang, F., Herzmark, P., Weiner, O. D., Srinivasan, S., Servant, G., and Bourne, H. R. (2002) Lipid products of PI(3)Ks maintain

persistent cell polarity and directed motility in neutrophils. *Nat. Cell Biol. 4*, 513−518.
(6) Czech, M. P. (2003) Dynamics of phosphoinositides in membrane retrieval and insertion. *Annu. Rev. Physiol. 65*, 791−815.
(7) DiNitto, J. P., Cronin, T. C., and Lambright, D. G. (2003) Membrane recognition and targeting by lipid-binding domains. *Sci. STKE*, re16.
(8) Corbin, J. A., Dirkx, R. A., and Falke, J. J. (2004) GRP1 pleckstrin homology domain: activation parameters and novel search mechanism for rare target lipid. *Biochemistry 43*, 16161−16173.
(9) Hennessy, B. T., Smith, D. L., Ram, P. T., Lu, Y., and Mills, G. B. (2005) Exploiting the PI3K/AKT pathway for cancer drug discovery. *Nat. Rev. Drug Discovery 4*, 988−1004.
(10) Hurley, J. H. (2006) Membrane binding domains. *Biochim. Biophys. Acta 1761*, 805−811.
(11) Hawkins, P. T., Anderson, K. E., Davidson, K., and Stephens, L. R. (2006) Signalling through Class I PI3Ks in mammalian cells. *Biochem. Soc. Trans. 34*, 647−662.
(12) Newton, A. C. (2009) Lipid activation of protein kinases. *J. Lipid Res. 50*, xxxx.
(13) Fayard, E., Xue, G., Parcellier, A., Bozulic, L., and Hemmings, B. A. (2010) Protein kinase B (PKB/Akt), a key mediator of the PI3K signaling pathway. *Curr. Top. Microbiol. Immunol. 346*, 31−56.
(14) Vadas, O., Burke, J. E., Zhang, X., Berndt, A., and Williams, R. L. (2011) Structural basis for activation and inhibition of class I phosphoinositide 3-kinases. *Sci. Signaling 4*, xxxx.
(15) Calleja, V., Laguerre, M., and Larijani, B. (2009) 3-D structure and dynamics of protein kinase B-new mechanism for the allosteric regulation of an AGC kinase. *J. Chem. Biol. 2*, 11−25.
(16) Calleja, V., Alcor, D., Laguerre, M., Park, J., Vojnovic, B., Hemmings, B. A., Downward, J., Parker, P. J., and Larijani, B. (2007) Intramolecular and intermolecular interactions of protein kinase B define its activation in vivo. *PLoS Biol. 5*, e95.
(17) Okuzumi, T., Fiedler, D., Zhang, C., Gray, D. C., Aizenstein, B., Hoffman, R., and Shokat, K. M. (2009) Inhibitor hijacking of Akt activation. *Nat. Chem. Biol. 5*, 484−493.
(18) Wu, W. I., Voegtli, W. C., Sturgis, H. L., Dizon, F. P., Vigers, G. P., and Brandhuber, B. J. (2010) Crystal structure of human AKT1 with an allosteric inhibitor reveals a new mode of kinase inhibition. *PLoS One 5*, e12913.
(19) Carpten, J. D., Faber, A. L., Horn, C., Donoho, G. P., Briggs, S. L., Robbins, C. M., Hostetter, G., Boguslawski, S., Moses, T. Y., Savage, S., Uhlik, M., Lin, A., Du, J., Qian, Y. W., Zeckner, D. J., Tucker-Kellogg, G., Touchman, J., Patel, K., Mousses, S., Bittner, M., Schevitz, R., Lai, M. H., Blanchard, K. L., and Thomas, J. E. (2007) A transforming mutation in the pleckstrin homology domain of AKT1 in cancer. *Nature 448*, 439−444.
(20) Lindhurst, M. J., Sapp, J. C., Teer, J. K., Johnston, J. J., Finn, E. M., Peters, K., Turner, J., Cannons, J. L., Bick, D., Blakemore, L., Blumhorst, C., Brockmann, K., Calder, P., Cherman, N., Deardorff, M. A., Everman, D. B., Golas, G., Greenstein, R. M., Kato, B. M., Keppler-Noreuil, K. M., Kuznetsov, S. A., Miyamoto, R. T., Newman, K., Ng, D., O'Brien, K., Rothenberg, S., Schwartzentruber, D. J., Singhal, V., Tirabosco, R., Upton, J., Wientroub, S., Zackai, E. H., Hoag, K., Whitewood-Neal, T., Robey, P. G., Schwartzberg, P. L., Darling, T. N., Tosi, L. L., Mullikin, J. C., and Biesecker, L. G. (2011) A mosaic activating mutation in AKT1 associated with the Proteus syndrome. *N. Engl. J. Med. 365*, 611−619.
(21) van den Wildenberg, S. M., Bollen, Y. J., and Peterman, E. J. (2011) How to quantify protein diffusion in the bacterial membrane. *Biopolymers 95*, 312−321.
(22) Jaskolski, F., and Henley, J. M. (2009) Synaptic receptor trafficking: the lateral point of view. *Neuroscience 158*, 19−24.
(23) Diaz, A. J., Albertorio, F., Daniel, S., and Cremer, P. S. (2008) Double cushions preserve transmembrane protein mobility in supported bilayer systems. *Langmuir 24*, 6820−6826.
(24) Qin, K., Sethi, P. R., and Lambert, N. A. (2008) Abundance and stability of complexes containing inactive G protein-coupled receptors and G proteins. *FASEB J. 22*, 2920−2927.
(25) Kenworthy, A. K. (2006) Fluorescence-based methods to image palmitoylated proteins. *Methods 40*, 198−205.
(26) Chen, Y., Lagerholm, B. C., Yang, B., and Jacobson, K. (2006) Methods to measure the lateral diffusion of membrane lipids and proteins. *Methods 39*, 147−153.
(27) Cezanne, L., Lopez, A., Loste, F., Parnaud, G., Saurel, O., Demange, P., and Tocanne, J. F. (1999) Organization and dynamics of the proteolipid complexes formed by annexin V and lipids in planar supported lipid bilayers. *Biochemistry 38*, 2779−2786.
(28) Tamm, L. K. (1988) Lateral diffusion and fluorescence microscope studies on a monoclonal antibody specifically bound to supported phospholipid bilayers. *Biochemistry 27*, 1450−1457.
(29) Knight, J. D., Lerner, M. G., Marcano-Velazquez, J. G., Pastor, R. W., and Falke, J. J. (2010) Single molecule diffusion of membrane-bound proteins: window into lipid contacts and bilayer dynamics. *Biophys. J. 99*, 2879−2887.
(30) Barth, A., Martin, S. R., and Bayley, P. M. (1998) Specificity and symmetry in the interaction of calmodulin domains with the skeletal muscle myosin light chain kinase target sequence. *J. Biol. Chem. 273*, 2174−2183.
(31) Yin, J., Straight, P. D., McLoughlin, S. M., Zhou, Z., Lin, A. J., Golan, D. E., Kelleher, N. L., Kolter, R., and Walsh, C. T. (2005) Genetically encoded short peptide tag for versatile protein labeling by Sfp phosphopantetheinyl transferase. *Proc. Natl. Acad. Sci. U. S. A. 102*, 15815−15820.
(32) Knight, J. D., and Falke, J. J. (2009) Single-molecule fluorescence studies of a PH domain: new insights into the membrane docking reaction. *Biophys. J. 96*, 566−582.
(33) Sbalzarini, I. F., and Koumoutsakos, P. (2005) Feature point tracking and trajectory analysis for video imaging in cell biology. *J. Struct. Biol. 151*, 182−195.
(34) Schutz, G. J., Schindler, H., and Schmidt, T. (1997) Single-molecule microscopy on model membranes reveals anomalous diffusion. *Biophys. J. 73*, 1073−1080.
(35) Goulian, M., and Simon, S. M. (2000) Tracking single proteins within cells. *Biophys. J. 79*, 2188−2198.
(36) Kasturi, R., Vasulka, C., and Johnson, J. D. (1993) Ca2+, caldesmon, and myosin light chain kinase exchange with calmodulin. *J. Biol. Chem. 268*, 7958−7964.
(37) Rayan, G., Guet, J. E., Taulier, N., Pincet, F., and Urbach, W. (2010) Recent Applications of Fluorescence Recovery after Photobleaching (FRAP) to Membrane Bio-Macromolecules. *Sensors (Basel) 10*, 5927−5948.
(38) Hardt, S. L. (1979) Rates of diffusion controlled reactions in one, two and three dimensions. *Biophys. Chem. 10*, 239−243.
(39) Weljie, A. M., Yamniuk, A. P., Yoshino, H., Izumi, Y., and Vogel, H. J. (2003) Protein conformational changes studied by diffusion NMR spectroscopy: application to helix-loop-helix calcium binding proteins. *Protein Sci. 12*, 228−236.
(40) Stahelin, R. V. (2009) Lipid binding domains: more than simple lipid effectors, *J. Lipid Res.* 50 Suppl, S299−304.
(41) Lietzke, S. E., Bose, S., Cronin, T., Klarlund, J., Chawla, A., Czech, M. P., and Lambright, D. G. (2000) Structural basis of 3-phosphoinositide recognition by pleckstrin homology domains. *Mol. Cell 6*, 385−394.
(42) Zhang, M., Tanaka, T., and Ikura, M. (1995) Calcium-induced conformational transition revealed by the solution structure of apo calmodulin. *Nat. Struct. Biol. 2*, 758−767.
(43) Gsponer, J., Christodoulou, J., Cavalli, A., Bui, J. M., Richter, B., Dobson, C. M., and Vendruscolo, M. (2008) A coupled equilibrium shift mechanism in calmodulin-mediated signal transduction. *Structure 16*, 736−746.
(44) Klee, C. B., Crouch, T. H., and Krinks, M. H. (1979) Calcineurin: a calcium- and calmodulin-binding protein of the nervous system. *Proc. Natl. Acad. Sci. U. S. A. 76*, 6270−6273.